

A Neural Network Separation Approach for the Inclusion of Static Friction in Nonlinear Static Models of Industrial Robots

Mojtaba A. Khanesar, Minrui Yan, Wahyudin P. Syam, Samanta Piano, Richard Leach, and David Branson

Abstract— Static friction modelling is a critical task to have an accurate robot model. In this paper, a neural network separation approach to include nonlinear static friction in models of industrial robots is proposed. For this purpose, the terms corresponding to static friction within the overall robot mathematical model are separable terms treated independently from the rest of the model. The separation modelling process is accomplished by first determining the mathematical model for the system by excluding the friction terms and estimating its parameter values. This part of the model corresponds to gravitational terms only. Because persistency of excitation is required to maintain high accuracy and avoid singularity in the estimations, data with large variations across multiple joint angles are gathered for estimation purposes and a weighted least-squares approach is used. This estimation results in a highly accurate static mathematical model for industrial robots. Results from the weighted least-squares estimation are compared to the original least-squares estimation, ridge regression, a least absolute shrinkage and selection operator, and an elastic net to show superior performance. After modelling the gravitational terms of the model, a multilayer perceptron neural network is used to identify static friction forces in the model from experimental data. This is required in the case of a robot with multiple degrees of freedom because the friction of each joint is a function of several other joint angles acting upon it; making the solution complex and difficult to be obtained through other friction modelling methods. Experimental results obtained from a Universal Robots-UR5 demonstrate the high accuracy of the proposed modelling methodology under static conditions, and future work will consider the implementation of dynamic terms to integrate friction forces during movement.

Index Terms— Estimation, friction, mathematical model, modeling, neural network model, robot

¹Manuscript received 2022-05-11;

This work is primarily funded and supported by the Engineering and Physical Sciences Research Council (EPSRC) under grant number: EP/T023805/1—High-accuracy robotic system for precise object manipulation (HARISOM).

(Corresponding author: M. A. Khanesar.)

Digital Object Identifier xx.xxxx/XXXX.xxx.xxxxxxxx

M. A. Khanesar, Minrui Yan, Samanta Piano, Richard Leach, and David Branson are with the Faculty of Engineering, University of Nottingham, Nottingham NG7 2RD, email: Mojtaba.Ahmadiehkhanesar@nottingham.ac.uk. Wahyudin P. Syam is with GMV UK, Sir Colin Campbell Building, Innovation Park, Triumph Road, Nottingham, NG7 2TU, United Kingdom.

I. INTRODUCTION

INDUSTRY 4.0 requires increasing levels of accuracy, and reliability of industrial robots to accomplish highly accurate production [1, 2]. To develop reliable control strategies and increase precision, it is required to have a robot model [3-6] that avoids excess rated torques and forces, predicts wear and tear, and avoids premature failures [7]. Friction [8], which inherently exists in the robot structure, is of high importance to maintain modelling accuracy and its inclusion in static robot models can reduce uncertainty resulting in more accurate overall motion.

Kinesthetic teaching mode which may be referred to as lead through programming mode is a very flexible teaching mode to program industrial robot motion [9]. This mode allows us to retrain robots on the factory floor with minimal operator knowledge about programming [10, 11], as the user simply guides the robot with their hand to record the required motions. Such teaching mode which exists in most cobots [12] - robots that can operate with humans collaboratively - are increasing their use in Industry 4.0 environments for handling and manipulating materials, packaging purposes [13] and teleoperation tasks [14]. These teaching modes are mostly utilized in Industry 4.0 environments where dynamic reskilling of robots on the factory floor is required to meet highly customizable products. Although, the inherent design characteristics of these teaching modes enable safe use, and generally increase compliance, it increases static friction effects in controlled joints.

To control industrial robots precisely and easily in kinesthetic teaching modes, it is required to determine the force to compensate for gravity and friction forces. For the kinesthetic modes of operation for an Effort ER20 C10, a heavy-duty industrial robot with 20 kg of mass, a force following controller was used to allow the robot to follow external forces applied by a human teacher [11]. These force following controllers relied highly on the mathematical model of the robot and its parameter values need to be precise. Even a small mismatch between the model and the robot may result in controller overcompensations, and consequently in unwanted motion [15]. Some industrial robots benefit from gravitational force and torque compensation by adding mechanical parts such as counterweights and springs [16]. However, such elements do not usually exist on most industrial robots, as they necessitate

the use of software for nonlinear gravity compensation and mechanical hardware, adding unwanted complexity and cost. A software feedback control loop based on dynamic models is, therefore, the preferable choice to improve position control [17]. To have an efficient and high-performance software antigravity control in industrial robots, it is required to have a precise separation approach to improve the industrial robot models in their static condition to better include static friction.

When a force is applied to a moving object, there is a Coulomb friction, proportional to the perpendicular force applied to the contact plane, and acting against the movement of the object [18]. An object can move in three states: adhesion or stick state, stick to slip state, and slip state. In the adhesion or stick state, the applied force is weaker than the Coulomb friction and the object remains still. During the stick to slip transition, the time dependent static friction avoids object movement [8]. However, when the object starts moving (slip state), the friction is a function of angular velocity. The Karnopp friction model considers friction for the system for all three states of stick, stick to slip transition and slip state [8]. Although Karnopp model has the advantage of using ordinary differential equations, it suffers from numerical instability in the stick mode. To overcome the numerical instability problem of a Karnopp friction model in stick mode, switch models may be used [8]. In the switch model, at each time instance, system states are inspected, and appropriate time derivatives of the states are chosen from the differential equations corresponding to stick phase, stick to slip phase or slip phase of operation. The seven-parameter friction model [19], the Dahl model [20], the LuGre model [21], the Leuven integrated friction model [22], and the generalized Maxwell slip model [23] are among the most popular ones used in the literature for friction modelling [24]. One issue is that such models are often concerned with low, typically single degree of freedom robots, while industrial robots tend to have many degrees of freedom (DoF) of motion. The focus of this paper is, therefore, on the static friction of industrial robots in their stick mode of operation, considering multiple joint angles and their interactions.

While dynamic friction is usually a function of angular velocities [25-30], static friction mostly relies on robot joint angles. The calculation of the static friction is especially important when operating using the kinesthetic mode. In general, to calculate the static friction of an industrial robot in [25], its speed is kept constant. For the kinesthetic mode of operation for an Effort ER20 C10, a heavy-duty industrial robot with 20 kg of mass, a force following controller is used to make the robot follow external forces applied by a human teacher [11]. These force following controllers rely heavily on the mathematical model of the robot and its estimated parameters. Due to unknown mathematical relationships between static friction and joint angles, artificial neural networks (ANNs) are used to model this relationship.

ANNs offer a solution to static friction modelling as they are general function approximators capable of picking up static friction as a smooth nonlinear function of joint angles, even though the real mathematical model is unknown. ANNs have already been used in a variety of friction modelling applications

for sliding surfaces and hydraulic actuators [31-34]. In the case of friction models in robotic applications, a neural network structure optimized by a genetic algorithm is used in [35] to model the joint friction for a single joint of a HSR JR605-C robot. It is observed that relatively large errors exist in the Stribeck model at low speeds [35]. To overcome large error in Stribeck models at low speeds due to static friction, a neural network optimized by a genetic algorithm was used leading to small mean squared errors for position tracking [35]. The robotic system investigated in [36] is a typical planar 1-degree of freedom rotating link robot with encoder feedback driven by a DC motor and a gear box. A support vector machine network approach is used to model friction in this robot [36]. Despite the existence of different friction models, a static friction model that considers systems with high DoF has not been studied.

In this paper, motivated by the fact that static friction for robots with high DoF has not been investigated, a separation approach is presented for the modelling of an industrial robot, in our case a Universal Robots-UR5, in its static state. First, the nonlinear gravity terms of the UR5 are modelled mathematically without considering static friction. Mathematical modelling that achieves results traceable to physical parameters of the robot is the preferred method for nonlinear gravity terms compared to fuzzy approaches [37] or neural network methods [33]. This provides more in-depth information about an industrial robot's dynamics that can be used in model-based control systems with greater accountability to what is occurring. Previous attempts to model this robot require simplification of its structure to calculate the inertia tensors of the robot links and centres of gravity. However, because of irregularities in the shapes of the robot links and manufacturing tolerances, such a mathematical model includes uncertainty. For instance in [38], the shapes of the robot links are considered completely cylindrical to extract the inertia tensor as well as centres of gravity. Because the proposed approach in this paper deals with real data gathered from the robot, it does not include the simplifications previously used in [38]. Euler-Lagrange method is the preferred approach in this paper to obtain industrial robot dynamic motion. The angular velocity and acceleration terms are taken as equal to zero during the mathematical modelling formulation process to find the static robot model. The parameter values of the robot static model are estimated from the real data, rather than a simplified robot structure, which makes them more precise.

Sparse identification of nonlinear dynamics (SINDY) is a system identification approach to reduce the modelling complexity and make it suitable for model-based control and simulation [39]. Inspired by its successful implementation, the regression methods used within this approach, including weighted least-squares (WLS) [7, 40], LASSO, ElasticNet and ridge regression, are used for parameter estimation of a gravitational model within the static robot model. Motivated by the fact that the aforementioned algorithms are used for dynamic system identification [39], this work uses these regression algorithms to estimate the parameters of the regression part of the robot static model. It is shown in the paper

that using the WLS technique results in a more accurate model than LASSO, ElasticNet and ridge regression.

Because of the high interaction between multiple robot links, the static friction terms corresponding to each joint are found to be dependent upon more than one joint. Therefore, the static friction terms are estimated using an appropriate neural network model as a function of joint angles J_2 , J_3 and J_4 (see Fig. 1). It is shown that the combination of the mathematical model for gravitational terms and the neural networks for friction models contributes to a precise and reliable model with negligible error. The systematic friction model developed in this study is assumed to account for the stick mode of the robot, which to the best of our knowledge has not been conducted before on these many joints. In summary the contributions of this paper are as summarized below.

- Introduction of a new “separation approach” to include static friction terms for the stick state of a robot static model. The separation approach introduced in the paper makes it possible to treat the static friction terms completely independent from the mathematical industrial robot model. Therefore, not only the developed model is capable of modelling static behavior of the robot with high accuracy as a result of using ANN in its structure, but also it provides mathematical model of gravitational force which are minimal and provides detailed physical static robot model.
- Use of WLS for the estimation of the gravitational term parameters to obtain a simple and accurate mathematical model. WLS algorithm is a successful estimation algorithm to deal with noise and uncertainties which exist in industrial robot data.
- Modelling the static friction terms using a neural network to increase accuracy in a multi-joint system. To the best of the author’s knowledge, static friction modelling for multiple robot joints does not exist in literature.

This paper is organized as follows. A dynamic model for industrial robots is presented in Section II. The model is then reduced to a static one to perform the parameter estimation. Estimation algorithms of ridge regression, LASSO, ElasticNet and WLS are explained in Section III, where the overall separation approach is given. Section IV presents the estimation results using the proposed approach and validates them experimentally. Concluding remarks are given in Section V.

II. INDUSTRIAL ROBOT DYNAMIC MODEL

The process of industrial robot model identification from data requires data acquisition, signal conditioning, structural identification, parameter estimation and finally model verification [41]. The data gathered for identification purposes needs to be in a persistently excited signal to avoid singularities in the estimation process. To maintain high excitation for the signal, large variations on multiple robot joint angles are considered. Another reason for having large variations in the signal is to have a precise model across a larger number of operational points [42]. In this work, the ordinary differential

equations that govern robot motion are obtained using Euler-Lagrange method. This Euler-Lagrange method uses the principle of “virtual work” to derive a mathematical model of the robot in terms of second order differential equations corresponding to each link [43].

Figure 1 illustrates the UR5 robot as a typical 6-DOF industrial robot, with six links connected to each other by revolute joints. The joint labels are presented using J_i , $i = 1, \dots, 6$, where J_1 is the shoulder pan joint, J_2 is the shoulder lift joint, J_3 is the shoulder elbow joint, J_4 is wrist joint 1, J_5 is wrist joint 2 and J_6 is wrist joint 3. The d_i , $i = 1, 4, 5, 6$ and a_i , $i = 2, 3$ parameters in Fig. 1, refer to the Denavit–Hartenberg (DH) parameters of UR5.

A. Physical Characteristics of Industrial Robot

The symbolic representation of inertia matrices and the centre of gravity for each link of the UR5 are as follows

$$I_k = \text{diag}(I_{1,1}^k \quad I_{2,2}^k \quad I_{3,3}^k), k = 1, \dots, 6 \quad (1)$$

where I_1, \dots, I_6 represent the inertia matrixes of link 1, ..., 6, respectively. During the modelling process in this paper, the off-diagonal terms in I_k are considered as equal to zero. The centre of mass corresponding to each link is represented by $r_{M_k}^k$, $k=1, \dots, 6$ and can be written as

$$\begin{aligned} r_{M_k}^k &= [0 \quad , \quad r_{M_k,2}^k, \quad r_{M_k,3}^k \quad]^T, k = 1, 4, 5, \\ r_{M_k}^k &= [r_{M_k,1}^k \quad , \quad 0, \quad r_{M_k,3}^k \quad]^T, k = 2, 3, \\ r_{M_6}^6 &= [0 \quad , \quad 0, \quad r_{M_6,3}^6 \quad]^T. \end{aligned} \quad (2)$$

rotation matrices for its joints as a function of joint angles [42, 44]. The parameters $r_{M_k,1}^k$, $k = 1, 4, 5$, $r_{M_k,3}^k$, $k = 2, 3$, and $r_{M_6,1}^6$, and $r_{M_6,2}^6$ are taken as equal to zero during the modelling process. In other words, it is assumed that the center of the mass in certain directions is exactly in the middle of the axis and its uncertainty is ignorable.

$$x = T_6^0 = T_1^0 T_2^1 T_3^2 T_4^3 T_5^4 T_6^5 = \begin{bmatrix} R_6^0 & o_6^0 \\ \mathbf{0} & 1 \end{bmatrix} \quad (3)$$

where,

$$T_i^{i-1} = \begin{bmatrix} cq_i & -sq_i c\alpha_i & sq_i s\alpha_i & a_i cq_i \\ sq_i & cq_i c\alpha_i & -cq_i s\alpha_i & a_i sq_i \\ 0 & s\alpha_i & c\alpha_i & d_i \\ 0 & 0 & 0 & 1 \end{bmatrix}, \quad (4)$$

and x represents the translation and rotation matrix relative to the base coordinate, q_i 's represent the joint angles, α_i 's and d_i 's represent the Denavit-Hartenberg (DH) parameters of the robot [45, 46]. The terms sq_i , $s\alpha_i$, cq_i and $c\alpha_i$ refer to $\sin(q_i)$, $\sin(\alpha_i)$, $\cos(q_i)$ and $\cos(\alpha_i)$ terms, respectively; these are the simplified representations of $\sin(\cdot)$ and $\cos(\cdot)$ functions throughout the paper. The positions of each link can be obtained

using the coordinate of the previous link using the rotation

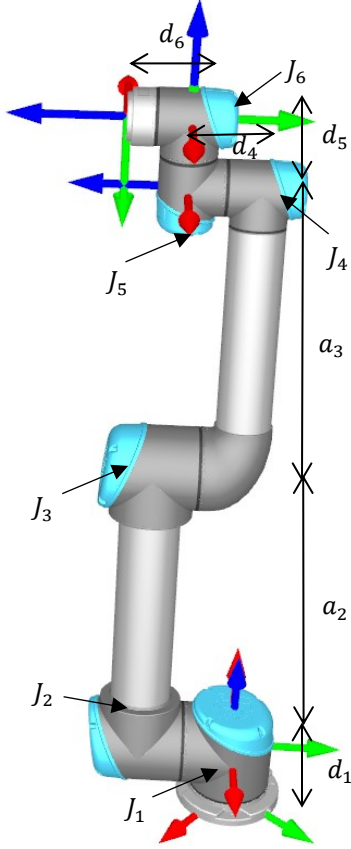


Fig. 1. Typical industrial robot (UR5) schematics ($d_i, i = 1, 4, 5, 6$ and $a_i, i = 2, 3$ parameters refer to the DH parameters of the UR5)

matrix R_{j-1}^i

$$d_j^i = d_{j-1}^i + R_{j-1}^i d_j^{i-1} \quad (5)$$

The linear and angular velocities of the end effector are related to the joint velocities and include the Jacobian of the forward kinematics of the robot as follows

$$\dot{X} = \begin{bmatrix} \dot{O}_n^0(q) \\ \dot{\beta}_n^0(q) \end{bmatrix} = \begin{bmatrix} V_n^0(q) \\ \dot{\beta}_n^0(q) \end{bmatrix} = J_a(q) \dot{q} \quad (6)$$

where $O_n^0(q)$ is the vector from the base frame origin to the end effector frame origin and $\beta_n^0(q) = [\varphi, \vartheta, \psi]^T$ denotes a representation for the orientation of the end effector frame relative to the base frame, and $J_a(q)$ is the Jacobian of the forward kinematics of the robot.

The total kinetic energy of the robot includes the angular velocity energy terms and the linear velocity terms and is given by: $K = \frac{1}{2} m v^T v + \frac{1}{2} m \omega^T J \omega$, where $J = R I R^T$. The kinetic energy of the system can then be modified as [19]

$$K = \frac{1}{2} \dot{q}^T M(q) \dot{q} = \frac{1}{2} \dot{q}^T \sum_{i=1}^n \{ m_i J_{v_{mi}}^T(q) J_{v_{mi}}(q) + J_{\omega_{mi}}^T(q) R_i(q) I_{mi}(q) R_i^T(q) J_{\omega_{mi}}(q) \} \dot{q} \quad (7)$$

where $R_i(q) \in \mathbb{R}^{3 \times 3}$ is the rotation matrix from the inertia frame to the body frame, $I_{mi}(q) \in \mathbb{R}^{3 \times 3}$ is the inertia tensor expressed in the body frame, m_i is the mass of link l_i , $I_{mi} \in \mathbb{R}^{3 \times 3}$ is the inertia tensor expressed in the body frame of link l_i , and $M(q) \in \mathbb{R}^{6 \times 6}$ is the positive definite inertia matrix of the manipulator.

To determine the potential energy of the robot, it is required to calculate the centre of gravity positions of the UR5 links in the frame attached to the base of UR5 as [43]

$$\begin{bmatrix} p_{c1} \\ 1 \end{bmatrix} = T_1^0 \begin{bmatrix} r_{M_1}^1 \\ 1 \end{bmatrix}, \begin{bmatrix} p_{c2} \\ 1 \end{bmatrix} = T_1^0 T_2^1 \begin{bmatrix} r_{M_2}^2 \\ 1 \end{bmatrix}$$

$$\begin{bmatrix} p_{c(k+1)} \\ 1 \end{bmatrix} = T_1^0 \dots T_{k+1}^k \begin{bmatrix} r_{M_{k+1}}^{k+1} \\ 1 \end{bmatrix}, k = 2, \dots, 5 \quad (8)$$

where the potential energy function of the UR5 is obtained from

$$P = \sum_{i=1}^6 m_i g^T p_{ci} \quad (9)$$

and p_{ci} is defined in equation (8). The Euler-Lagrange approach is used to model the dynamics of this system, where the dynamic equations governing the UR5 are obtained through the calculation of the partial derivative terms as $\frac{d}{dt} \left(\frac{\partial L}{\partial \dot{q}} \right) - \frac{\partial L}{\partial q} = \tau$ where τ presents the motor torque applied to each of industrial robot joints. Using the Lagrange function $L = K - P$ and considering that the potential energy depends on joint angles, but not joint speeds as this is static behavior, the Lagrange function can be written as

$$\frac{d}{dt} \left(\frac{\partial K}{\partial \dot{q}} \right) - \frac{\partial K}{\partial q} + \frac{\partial P}{\partial q} = \tau - \tau_f. \quad (10)$$

inertial forces *gravity vector*

Equation (10) can be further modified to obtain the vectoral second order dynamic equation governing the system

$$M(q) \ddot{q} + V(q, \dot{q}) + G(q) = \tau - \tau_f \quad (11)$$

where $M(q)$ is a positive definite inertia matrix of the manipulator defined previously in equation (7) and $\tau_f \in \mathbb{R}^{6 \times 1}$ presents the static friction vector on all joints of the industrial robot. The matrix $V(q, \dot{q})$ represents the centrifugal and Coriolis forces, which include the angular velocities, partial derivatives of $M(q)$ with respect to angular positions and the time derivative of $M(q)$, using the following

$$V(q, \dot{q}) = \dot{M} \dot{q} - \frac{1}{2} \left[\dot{q}^T \frac{\partial M}{\partial q_1} \dot{q} \quad \dots \quad \dot{q}^T \frac{\partial M}{\partial q_n} \dot{q} \right]^T \quad (12)$$

$G(q)$ is obtained using the partial derivatives of the potential energy $P(q)$ with respect to joint angles represented by $G(q) = \frac{\partial P(q)}{\partial q}$. Using equation (9), the term $G(q)$ can be manipulated to

give

$$G(q) = \frac{\partial P}{\partial q} = \sum_{i=1}^6 m_i g^T \frac{\partial p_{ci}}{\partial q} \quad (13)$$

III. METHODOLOGY

In this paper, we are considering a static model of industrial robots; for this reason, the angular velocities of the robot are considered negligible. Industrial robot static friction terms are separable from its mathematical model representing gravitational terms. Therefore, a separation approach is used to find the static friction terms. First, the parameters of the mathematical model of the robot are estimated. For this purpose, the static model of the system, excluding static friction, is formulated as a linear regression problem. After estimating the linear regression parameters, the remaining terms, related to the static friction, are identified as a function of joint angles using a neural network approach. Each step is explained in detail in the next sections.

A. Problem statement

The problem which is investigated in this paper is to model static motion behavior of industrial robot to maximize the advantage of using mathematics in the modelling. To this end, a mathematical formulation is used to identify gravity terms. Linear regression is then used to estimate parameters of the gravity terms. Because of the high level of interaction between different links and joints, the static friction acting on each joint will depend on multiple joint angles. Therefore, in this paper, multiple layer perceptron neural network (MLPNN) is used as a strong function approximator for static friction terms [47, 48]. With this approach the static friction function acting on each joint, in relation to the other joints, is identified.

B. Construct the regressor functions: the gravitational force term.

This section shows the procedure to determine the regressor functions which include gravitational force terms. We have the following equation for the gravitational force terms matrix $G(q)$

$$G(q) = [G_1(q) \quad G_2(q) \quad \dots \quad G_6(q)]^T \quad (14)$$

where $G_1(q) = 0$, $G_2(q) = \varphi_2(q)\theta_2$, $G_4(q) = \varphi_4(q)\theta_4$, $G_5(q) = \varphi_5(q)\theta_5$, $G_6(q) = 0$, $\theta_2 \in R^{5 \times 1}$, $\theta_3 \in R^{4 \times 1}$, $\theta_4 \in R^{3 \times 1}$, $\theta_5 \in R^{2 \times 1}$ are the unknown parameters of the system. $\varphi_2(q), \dots, \varphi_5(q)$ are then the known regressor values used for the regression algorithm to estimate system parameters calculated as

$$\varphi_2 = [\cos(q_2 + q_3)\cos(q_4)\sin(q_5), \cos(q_2 + q_3)\sin(q_4), \cos(q_2 + q_3), \cos(q_2), \sin(q_2 + q_3)\sin(q_4)\sin(q_5), \sin(q_2 + q_3)\cos(q_4)],$$

$$\varphi_3 = [\sin(q_2 + q_3 + q_4), \cos(q_2 + q_3), \cos(q_2 + q_3 + q_4)\sin(q_5)],$$

$$\varphi_4 = [\sin(q_2 + q_3 + q_4), \cos(q_2 + q_3 + q_4)\sin(q_5)],$$

$$\varphi_5 = [\sin(q_2 + q_3 + q_4)\cos(q_5)]. \quad (15)$$

Motor torque τ is considered in [38] and [49] as a linear function of motor current. However, in this paper the motor torque is considered as a polynomial function of motor current as nonlinear relationships were observed in the data. The motor torque-current relationship is, therefore, considered as

$$\tau_i = K_{2i}i_i^2 \text{sign}(i_i) + K_{1i}i_i + K_{0i} \quad (16)$$

where K_{0i}, K_{1i} and K_{2i} are the unknown parameters of UR5 motors. As the robot is operating in static mode, equation (11) can be simplified as follows

$$\begin{bmatrix} \varphi_2(q)\theta_2 & \varphi_3(q)\theta_3 & \dots & \varphi_5(q)\theta_5 \end{bmatrix}^T = \begin{bmatrix} \tau_2 - \tau_{f2} & \tau_3 - \tau_{f3} & \dots & \tau_5 - \tau_{f5} \end{bmatrix}^T \quad (17)$$

To estimate the robot regression parameters that appear in equation (16) initially the friction terms are not considered. After estimating the system parameters, excluding friction terms, using the linear regression approach, a neural network is used to identify the remaining terms related to the static friction terms. Each of the vector elements in equation (17) can be treated separately using the current-torque relationship as in equation (16)

$$\varphi_i(q)\theta_i = K_{2i}i_i^2 \text{sign}(i_i) + K_{1i}i_i + K_{0i} \quad (18)$$

Since the parameters of the motors K_{0i}, K_{1i} and K_{2i} are unknown, it is required to modify equation (18) to estimate them. Thus, equation (18) is modified as follows

$$\varphi_i(q)\theta_i/K_{1i} - K_{2i}i_i^2 \text{sign}(i_i)/K_{1i} - K_{0i}/K_{1i} = i_i. \quad (19)$$

Regression estimation methods are then applied to the augmented regressor vectors as follows

$$R_i(q) = [\varphi_i(q) \quad i_i^2 \text{sign}(i_i) \quad 1]. \quad (20)$$

Using equation (19), the regression problem in equation (17) can be rewritten as $R_i(q)\theta_i = i_i$, where θ_i s are vectors of the unknown parameters for the i -th joint as $\theta_i = [\theta_i^T \quad -K_{2i}/K_{1i} \quad -K_{0i}/K_{1i}]$.

B. Solving the regression problem: Estimation Methods

Different estimation algorithms including least squares, ridge regression, LASSO, elastic-net and WLS are discussed and are compared in terms of accuracy and the modelling complexity. The comparison criteria used for this work are the accuracy and speed of the algorithms. These methods are briefly presented in this section.

1) Least-squares method

The least-squares regression problem is frequently met in engineering applications and its cost function is expressed as [50, 51]

$$E_i(\theta_i) = \|R_i(q)\theta_i - i_i\|^2. \quad (21)$$

The solution to this problem is a Moore-Penrose pseudo inverse solution as $\theta_{i,LS} = (R_i^T R_i)^{-1} R_i^T i_i$. Although the pseudo inverse solution is the optimal solution to L_2 -norm of approximation error, reformulating the problem in the form of a ridge regression problem results in decreasing modelling complexity and avoids singularities.

2) Ridge Regression

Ridge regression benefits from a penalty term which tends to push the parameters of the system towards zero decreasing the modelling complexity. The cost function associated with this algorithm is

$$E_i(\theta_i) = \|R_i(q)\theta_i - i_i\|^2 + \frac{\alpha_1}{2} \|\theta_i\|^2 \quad (22)$$

and its solution is $\theta_{i,RR} = (R_i^T R_i + \alpha_1 I)^{-1} R_i^T i_i$ [50, 51]. The solution to ridge regression is biased with respect to optimal L_2 norm of approximation error. The value of the bias term is $\theta_{LS} - \theta_{RR} = \alpha_1 (R_i^T R_i)^{-1} (R_i^T R_i + \alpha_1 I)^{-1} R_i^T i_i$. Since the bias value generally increases as α_1 increases, values for α_1 that are too large should be avoided. Appropriate values for this parameter after a trial and error are found to be equal to 0.001.

3) LASSO

The cost function associated with LASSO includes L_1 -norm of system parameters as its penalty term is defined as [52], thus

$$E_i(\theta_i) = \|R_i(q)\theta_i - i_i\|^2 + \frac{\alpha_2}{2} \|\theta_i\|_1^2. \quad (23)$$

The L_1 -penalty term in the LASSO approach contributes to the reduction of the modelling complexity.

4) Elastic Net

The cost function associated with Elastic net is defined as follows [53]

$$E_i(\theta_i) = \|R_i(q)\theta_i - i_i\|^2 + \frac{\alpha_3}{2} \|\theta_i\|_1^2 + \frac{1-\alpha_3}{2} \|\theta_i\|^2. \quad (24)$$

This model benefits from a penalty term which is a convex sum of the penalty terms previously presented under LASSO and ridge regression.

5) Weighted Least Squares

The cost function for WLS benefits from a weight for each individual sample which may differ from each other as $E_i(\theta_i) = \|W_i^{1/2} (R_i(q)\theta_i - i_i)\|^2$, where W_i is selected as $W_i = [1/\sigma_1^2 \quad 1/\sigma_2^2 \quad \dots \quad 1/\sigma_N^2]$ and $\sigma_j^2, j = 1, \dots, N$ is the variance value associated with j -th sample [50, 51]. Therefore, estimation of the sample variances is required using orthogonal least squares, which is then used in a WLS algorithm.

C. Use MLP Neural Networks for Modelling Friction Terms

The neural network model used in this paper is a multilayer perceptron neural network (MLPNN), which is a popular type of neural network [54] as it is a general function approximator capable of dealing with a wide class of smooth functions. This network structure is composed of several units that perform mathematical tasks to calculate nonlinear function of the weighted sum of their inputs. In this paper, a hyperbolic tangent function is preferred because of its more frequent use and strong general function approximation capabilities for hidden layer activation functions [54]. The structure is a layered structure whose size can be increased by adding more layers and adding more neurons to each layer. This layered structure makes it possible to apply a gradient descent algorithm to train the network.

The residual of the regression analysis remaining after modelling the gravitational terms is the static friction terms which are a function of the four robot joints including: J_2 : shoulder lift joint, J_3 : shoulder elbow joint, J_4 : wrist joint 1, J_5 : wrist joint 2. Since the static friction function is unknown, MLPNN is used to estimate it. The residual terms remaining from the regression analysis are used as the target values for MLPNN which is implemented upon its input values. The training method for neural network model is a Levenberg-Marquardt method [55].

IV. RESULTS

To show the capability of the proposed approach to model industrial robots, the Universal Robots-UR5 is selected. The DH convention for UR5 uses four parameters to fully identify the motion coordinate of each link with respect to the previous link coordinates. The separation approach includes applying WLS to identify the gravity terms and then using MLPNN to identify static friction terms acting on industrial robot joints. The Regressors are generated using (20) which are then used to estimate gravity term parameters in a WLS algorithm. MLPNN is applied to the residual terms to identify static friction. The DH parameters of the robot appear within static industrial robot model which is identified within the static modelling process. However, according to the UR5 specifications provided by manufacturer [56] their nominal values are as presented in Table 1.

A. Experimental System Components

The experimental setup to test the proposed separation approach and estimate static friction in stick mode consists of the UR5 (see Fig. 2) with its teaching pendant and a PC running Ubuntu 18.04 connected to it via a LAN interface. The interface between the Ubuntu and the UR5 is realized through robot operating system (ROS) Melodic software¹. The specifications of the PC providing this connection are Intel Xeon CPU running at 3.5 GHz and 32 GB of RAM. The sampling frequency for gathering data using the ROS from the UR5 onboard sensors is 125 Hz. The ROS software can log the robot movements

¹ https://github.com/UniversalRobots/Universal_Robots_ROS_Driver (visited 17/05/2022)

directly to a comma-separated values (CSV) file structure readable through spreadsheet software, while the robot is performing different movements defined by the user on the teaching pendant. Data is available through a public research data webpage of the University of Nottingham [57].

For estimation purposes, numerous step movements to span whole wide range of working volume are required, affecting

TABLE 1
DH PARAMETERS AS WELL AS LINK WEIGHTS OF UR5

Parameter	Value (Kg)	Parameter	Value (mm)	Parameter	Value (mm)	Parameter	Value (rad)
M_1	3.7	a_1	0	d_1	89.16	α_1	$\pi/2$
M_2	8.393	a_2	-425	d_2	0	α_2	0
M_3	2.275	a_3	-392	d_3	0	α_3	0
M_4	1.219	a_4	0	d_4	109.15	α_4	$\pi/2$
M_5	1.219	a_5	0	d_5	94.65	α_5	$-\pi/2$
M_6	0.1879	a_6	0	d_6	82.3	α_6	0



Fig. 2 UR5 robot

several robot joints simultaneously to maintain high degrees of persistency of excitation. This is because a signal with a low degree of persistency of excitation may result in poor quality or even singularities in the estimation process. To ensure persistency of excitation in the data, large variations across multiple joints are considered. For measurement purposes, the UR5 is guided using its teaching pendant and measurements are performed in terms of joint angles, joint angular velocities, and joint currents using built-in sensors for the UR5 robot. ROS Melodic under Linux 18.04 is used for data collection purposes. Joint movements are assigned in a UR5 program with teaching pendant using 650 waypoints at maximum angular speed of 60°sec^{-1} and maximum angular acceleration of 80°sec^{-2} . There is at least a 95ms time delay between the movement commands which is required to have ten samples corresponding to static movements to perform static system identification. The total time it takes for the UR5 to travel all these waypoints is 4782 s. Figure 3 illustrates the raw data gathered from the UR5

in terms of joint angle data versus time.

B. Regression Results

In this paper, least-squares, ridge regression, Elastic Net, LASSO and WLS are used to estimate the model parameters for the system. The general structure of the model is obtained using the mathematical formulation presented in Section II-A. Because the model is investigated in steady state, when the angular velocities and accelerations are equal to zero, it is the steady state part of the signal needs to be determined. Then, ten consecutive samples from the steady state for each pose are used for estimation purposes. Least-squares, ridge regression, LASSO, Elastic Net, and WLS available under Python package `sklearn.linear_model` are used for the parameter estimation. Similar comparison between linear regression techniques has previously done in [58]. The software implementations are carried out under Spyder IDE. The

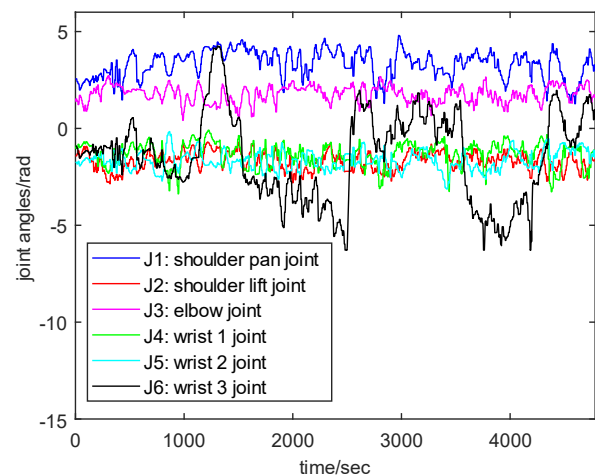


Fig. 3. Joint angle data gathered from UR5.

regressors used for estimation are those presented in equations (15) to (19). The targets considered for the six joints of the UR5 are the values of currents i_1 to i_6 , and correspond to motor torque values. The results obtained using WLS for θ_2 parameters are depicted in Fig. 4. The uncertainties associated with each individual estimated parameter are presented in the figure. Other than superior performance for WLS over other regression algorithms, it is easy to perform individual uncertainty analysis for each of the parameters in the model. This feature makes WLS a superior choice over other regression approaches studied in this paper.

Performance comparisons for the five algorithms are presented in Table 2. The parameter α_i , with $i = 1, 2, 3$, used in these estimations is selected as equal to 0.001. The tolerance of the calculations associated with Python IDE used in this paper is equal to $1e-8$. As can be seen from Table 1, the WLS method is the most accurate model among all estimation approaches.

Overall fitness results using the three algorithms when $\alpha_i, i = 1, 2, 3$, are equal to 0.001 are presented in Figure 5, where it is shown that using the mathematical model of the robot without the friction terms in the first stage results in modelling error (see Table 2). In the following section, the modelling residual is analyzed to find an appropriate MLPNN for the static friction.

C. Static Friction Modelling

The resulting residual of mathematical model for gravity terms is mainly due to static friction whose mathematical formulation is unknown. MLPNN is used to identify the friction force corresponding to each joint. The static friction term is not simply a function of joint angle θ , but of multiple joints. This is because the UR5 robot has multiple links and there is a significant interaction between them. Hence, a MLPNN is required to completely model the static friction terms of an UR5 robot model from the recorded data. The activation functions used for the layers in the MLPNN are linear, hyperbolic tangent sigmoid (TanSig), TanSig and linear for the four layers, respectively. For each friction function on a joint, a MLPNN is considered. To find the best MLPNN structure, several tests are performed. 75% of data is selected for training, 20% for testing, and 5% of data for validation

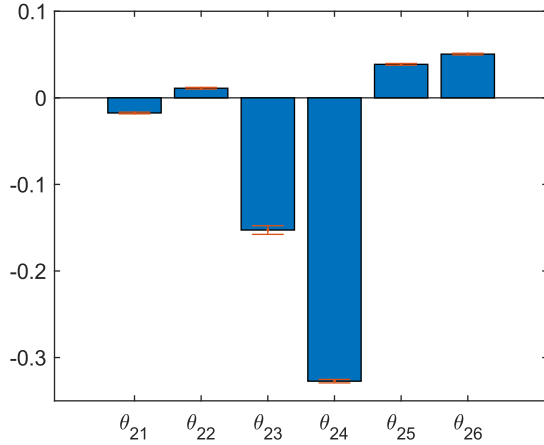


Figure 4 parameters associated with gravity terms for joint angle #2 (θ_2) estimated using WLS and their associated uncertainty analysis

TABLE 2
PERFORMANCE OF THE FIVE ESTIMATION METHODS

METHOD	LEAST SQUARES	RIDGE REGRESSION	LASSO	ELASTIC NET	WLS
RMSE	0.086	0.086	0.090	0.094	0.086

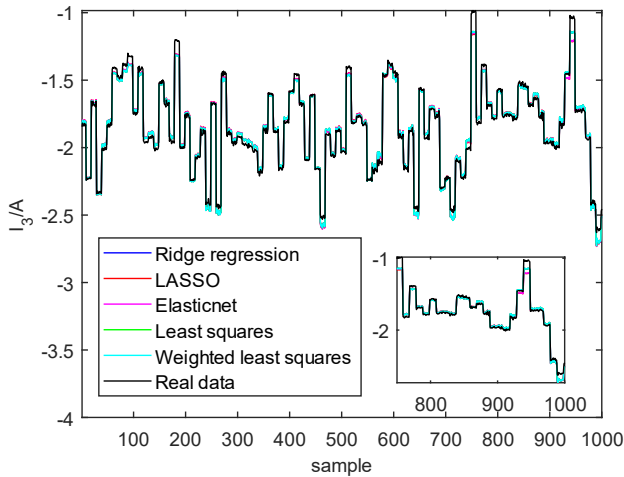


Figure 5. Estimated motor currents versus real motor currents collected from data for shoulder pan joint.

purposes. The input values to these MLPNNs are joint angles #2-#5 and the output values are each of the friction functions corresponding to each joint. A Levenberg-Marquardt estimation method is used to estimate the parameters of MLPNN with 1,000 epochs. The software package used for the MLPNN training purposes is pyrenn available under Python. `train_LM` attribute under this software package is used to apply Levenberg-Marquardt (LM) to MLPNN. The adaptive parameter within LM is decreased after each successful step and is only increased after a tentative step would increase the training cost function [59]. In this way, the performance function is always reduced at each iteration resulting in its convergence [42]. Table 3 summarizes MLPNN structure selection test results. Using this analysis, the optimal number of hidden layers is selected as equal to 3, and the optimal number of neurons in layers is selected as equal to 4-20-20-10-1. The RMSE for the validation data for this structure is equal to 0.008 which validates the whole identification process.

The regression analysis for identification in the third joint is illustrated in Fig. 7. The target value for this regression analysis shown on the abscissa is I_3 , the third joint motor current, and its approximate value appears on the ordinate. As can be seen in Fig. 7, the R-number is very close to unity for both train and test datasets. The overall identification performance of the proposed approach, which benefits from the mathematical model plus MLPNN for all joints, is presented in Table 4. The results show that the proposed approach successfully models the industrial robot in its static behaviour. The training RMSEs for the first two joints J_1 and J_2 are slightly higher than for the remaining joints. This is mainly because they are acting as the main lifting joints and are therefore affected more by other joints forces and torques. The overall RMSEs are relatively low and thus accuracy is maintained.

The output of the proposed model for all friction terms are depicted in Fig. 8. As can be seen from this figure, the overall static system model, including the mathematical terms and MLPNN for the system, demonstrates high accuracy. Hence, the separation approach proposed in this study can be used as a mathematical modelling approach to include friction terms in industrial robot static models such as that of the UR5.

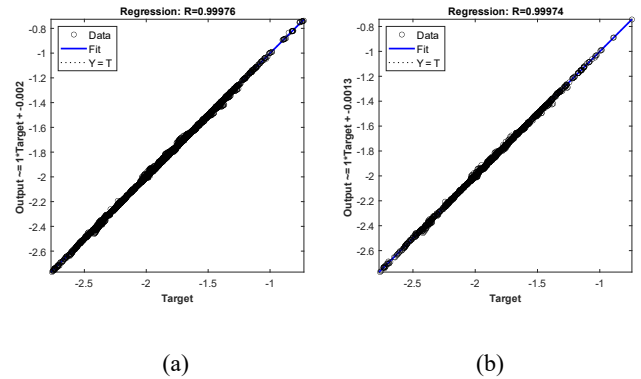


Figure 7. Regression analysis for overall static friction in J_3 for a) train data b) test data

V. CONCLUSIONS AND FUTURE WORKS

In this paper, a neural network separation approach is

developed to find the static model of an industrial robot, where the resulting model has friction terms in addition to the gravitational force terms. The gravitational force terms are formulated as a regression problem. To solve this regression problem, comparison results of several estimation algorithms including least-squares, ridge regression, elastic net, LASSO and WLS are presented. The WLS approach is found to be the preferred method to estimate gravitational terms as it results in an accurate mathematical model for the static motion of

TABLE 3
IDENTIFICATION ERRORS CORRESPONDING TO DIFFERENT MLPNNs

Number of neurons in layers	Number of hidden layers	Train	Test
4,20,10,10,1	3	0.0337	0.0314
4,10,10,1	2	0.1068	0.0694
4,20,10,1	2	0.0546	0.0524
4,15,10,1	2	0.0610	0.0586
4,20,15,10,1	3	0.0162	0.0140
4,15,15,10,1	3	0.0266	0.0228
4,10,10,10,1	3	0.0550	0.0521
4,20,20,10,1	3	0.0084	0.0073

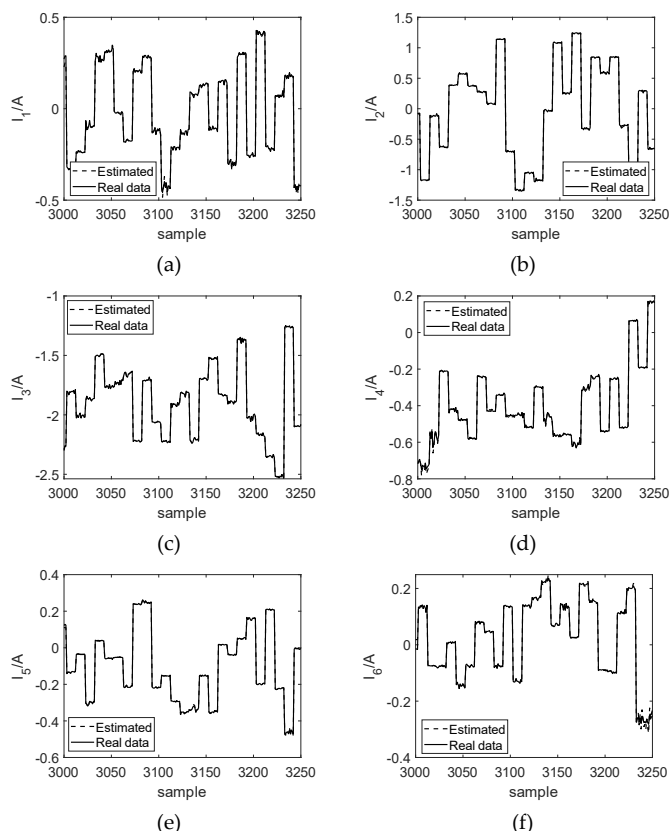


Figure 8. Modelling performance of static model for (a) shoulder pan joint (b) shoulder lift joint (c) shoulder elbow joint (d) wrist 1 joint (e) wrist 2 joint (f) wrist 3 joint.

TABLE 4
IDENTIFICATION ERRORS OF THE PROPOSED APPROACH ON EACH JOINT

Joint name / number	RMSE value	
	Train data	Test data
shoulder pan joint / #1	0.009	0.010
shoulder lift joint / #2	0.009	0.010
shoulder elbow joint / #3	0.003	0.003
wrist 1 joint / #4	0.008	0.011
wrist 2 joint / #5	0.006	0.007
wrist 3 joint / #6	0.007	0.007

industrial robots. Once the regression part of the static model, excluding static friction, had been derived, we further determined the static friction terms using a MLPNN. The overall combination of the gravitational terms model and the neural network model for the friction term is shown to result in an accurate model for the system. Results from this work will enable increased accuracy of industrial robot systems operating at static conditions, with future work seeking to consider the inclusion of dynamic motion behavior for industrial robots using the separation approach investigated in this paper.

As a future work dynamic modelling [52] of industrial robots will be investigated where different dynamic identification techniques such as deep learning [60], and state transition algorithm [61] may be utilized. The static robot model can be used to guide the robot to the desired position, disturbance rejection is added through the dynamic controller to maintain the robot position. Moreover, calculating the optimal rest position of industrial robots will be considered as future work. There exist two types of mechanisms to stop robots in their rest state: permanent magnet brakes and spring-set brakes². To find out the optimal rest position of an industrial robot to decrease its joint brakes wears, it is required to study the full static model of an industrial robot including its gravitational force terms and static friction model. As a future work using the proposed industrial robot static model in this paper, optimal rest position of the robot to minimize the torque applied to the joint brakes will be considered.

VI. ACKNOWLEDGMENT

This work is primarily funded and supported by the Engineering and Physical Sciences Research Council (EPSRC) under grant number: EP/T023805/1—High-accuracy robotic system for precise object manipulation (HARISOM). The authors would also like to thank the UKRI Research England Development (RED) Fund for partial funding this work via the Midlands Centre for Data-Driven Metrology.

VII. REFERENCES

- [1] P. Burnap *et al.*, "Chatty factories: A vision for the future of product design and manufacture with IoT," 2019.
- [2] A. Bueno, M. Godinho Filho, and A. G. Frank, "Smart production planning and control in the Industry 4.0 context: A systematic

² <https://blog.robotiq.com/whats-the-best-position-to-store-your-robot-overnight>

- literature review," *Computers & Industrial Engineering*, vol. 149, p. 106774, 2020.
- [3] X. Zheng, M. Xiong, R. Tian, J. Zheng, M. Wang, and G. Xie, "Three-Dimensional Dynamic Modeling and Motion Analysis of a Fin-Actuated Robot," *IEEE/ASME Transactions on Mechatronics*, 2022.
- [4] M. M. Alam *et al.*, "Inclusion of Bidirectional Angular Positioning Deviations in the Kinematic Model of a Six-DOF Articulated Robot for Static Volumetric Error Compensation," *IEEE/ASME Transactions on Mechatronics*, 2022.
- [5] Y. Wang, J. Wang, and Y. Fei, "Design and modeling of tetrahedral soft-legged robot for multi-gait locomotion," *IEEE/ASME Transactions on Mechatronics*, 2021.
- [6] Y. Liu, T. G. Mohanraj, M. R. Rajebi, L. Zhou, and F. Alambeigi, "Multiphysical Analytical Modeling and Design of a Magnetically Steerable Robotic Catheter for Treatment of Peripheral Artery Disease," *IEEE/ASME Transactions on Mechatronics*, 2022.
- [7] Y. Han, J. Wu, C. Liu, and Z. Xiong, "An iterative approach for accurate dynamic model identification of industrial robots," *IEEE Transactions on Robotics*, vol. 36, no. 5, pp. 1577-1594, 2020.
- [8] R. Leine, D. Van Campen, A. De Kraker, and L. Van Den Steen, "Stick-slip vibrations induced by alternate friction models," *Nonlinear dynamics*, vol. 16, no. 1, pp. 41-54, 1998.
- [9] S. L. Canfield, J. S. Owens, and S. G. Zuccaro, "Zero Moment Control for Lead-Through Teach Programming and Process Monitoring of a Collaborative Welding Robot," *Journal of Mechanisms and Robotics*, vol. 13, no. 3, p. 031016, 2021.
- [10] J. J. Steil, C. Emmerich, A. Swadzba, R. Grünberg, A. Nordmann, and S. Wrede, "Kinesthetic teaching using assisted gravity compensation for model-free trajectory generation in confined spaces," in *Gearing Up and Accelerating Cross-fertilization between Academic and Industrial Robotics Research in Europe*:: Springer, 2014, pp. 107-127.
- [11] S. Zhang, S. Wang, F. Jing, and M. Tan, "A sensorless hand guiding scheme based on model identification and control for industrial robot," *IEEE Transactions on Industrial Informatics*, vol. 15, no. 9, pp. 5204-5213, 2019.
- [12] E. Romiti *et al.*, "Toward a Plug-and-Work Reconfigurable Cobot," *IEEE/ASME Transactions on Mechatronics*, 2022.
- [13] D. Schaefer and W. M. Cheung, "Smart packaging: opportunities and challenges," *Procedia Cirp*, vol. 72, pp. 1022-1027, 2018.
- [14] A. Ghosh, D. A. P. Soto, S. M. Veres, and A. Rossiter, "Human robot interaction for future remote manipulations in industry 4.0," *IFAC-PapersOnLine*, vol. 53, no. 2, pp. 10223-10228, 2020.
- [15] M. A. Khanesar, O. Kaynak, and E. Kayacan, *Sliding-Mode Fuzzy Controllers*. Springer, 2021.
- [16] V. Arakelian, "Gravity compensation in robotics," *Advanced Robotics*, vol. 30, no. 2, pp. 79-96, 2016.
- [17] W. Montalvo, J. Escobar-Naranjo, C. A. Garcia, and M. V. Garcia, "Low-cost automation for gravity compensation of robotic arm," *Applied Sciences*, vol. 10, no. 11, p. 3823, 2020.
- [18] J. Swevers, W. Verdonck, and J. De Schutter, "Dynamic model identification for industrial robots," *IEEE control systems magazine*, vol. 27, no. 5, pp. 58-71, 2007.
- [19] B. Armstrong-Hélouvy, P. Dupont, and C. C. De Wit, "A survey of models, analysis tools and compensation methods for the control of machines with friction," *Automatica*, vol. 30, no. 7, pp. 1083-1138, 1994.
- [20] P. R. Dahl, "A solid friction model," Aerospace Corp El Segundo Ca, 1968.
- [21] C. C. De Wit, H. Olsson, K. J. Astrom, and P. Lischinsky, "A new model for control of systems with friction," *IEEE Transactions on automatic control*, vol. 40, no. 3, pp. 419-425, 1995.
- [22] J. Swevers, F. Al-Bender, C. G. Ganseman, and T. Projogo, "An integrated friction model structure with improved presliding behavior for accurate friction compensation," *IEEE Transactions on automatic control*, vol. 45, no. 4, pp. 675-686, 2000.
- [23] F. Al-Bender, V. Lampaert, and J. Swevers, "The generalized Maxwell-slip model: a novel model for friction simulation and compensation," *IEEE Transactions on automatic control*, vol. 50, no. 11, pp. 1883-1887, 2005.
- [24] V. Van Geffen, "A study of friction models and friction compensation," ed: Technische Universiteit Eindhoven Eindhoven (Holland, 2009.
- [25] A. C. Bittencourt and S. Gunnarsson, "Static friction in a robot joint—modeling and identification of load and temperature effects," *Journal of Dynamic Systems, Measurement, and Control*, vol. 134, no. 5, 2012.
- [26] R. Waiboer, "Dynamic modelling, identification and simulation of industrial robots," *Diss. University of Twente [Host]*, 2007.
- [27] L. Ding, H. Wu, Y. Yao, and Y. Yang, "Dynamic model identification for 6-DOF industrial robots," *Journal of Robotics*, vol. 2015, 2015.
- [28] M. Gautier and S. Briot, "Dynamic parameter identification of a 6 DOF industrial robot using power model," in *2013 IEEE International Conference on Robotics and Automation*, 2013: IEEE, pp. 2914-2920.
- [29] Z. Fu *et al.*, "A Lie theory based dynamic parameter identification methodology for serial manipulators," *IEEE/ASME Transactions on Mechatronics*, 2020.
- [30] C. Gaz, M. Cognetti, A. Oliva, P. R. Giordano, and A. De Luca, "Dynamic identification of the franka emika panda robot with retrieval of feasible parameters using penalty-based optimization," *IEEE Robotics and Automation Letters*, vol. 4, no. 4, pp. 4147-4154, 2019.
- [31] T. Nasir, B. Yousif, S. McWilliam, N. Salih, and L. Hui, "An artificial neural network for prediction of the friction coefficient of multi-layer polymeric composites in three different orientations," *Proceedings of the Institution of Mechanical Engineers, Part C: Journal of Mechanical Engineering Science*, vol. 224, no. 2, pp. 419-429, 2010.
- [32] Y. L. Karnavas and A. Vairis, "Modelling Of Frictional Phenomena Using Neural Networks: Friction Coefficient Estimation," *Proc. Of the IASTED Int. Conf. Applied Simulation and Modelling (ASM 2011)*, pp. 54-58.
- [33] L. Márton and S. Fodor, "Neural Network-based Friction Identification in Hydraulic Actuators."
- [34] A. Serafińska, W. Graf, and M. Kaliske, "Artificial Neural Networks Based Friction Law for Elastomeric Materials Applied in Finite Element Sliding Contact Simulations," *Complexity*, vol. 2018, 2018.
- [35] X. Tu, Y. Zhou, P. Zhao, and X. Cheng, "Modeling the static friction in a robot joint by genetically optimized BP neural network," *Journal of Intelligent & Robotic Systems*, vol. 94, no. 1, pp. 29-41, 2019.
- [36] G. Wang, Y. Li, and D. Bi, "Support vector machine networks for friction modeling," *IEEE/ASME Transactions on Mechatronics*, vol. 9, no. 3, pp. 601-606, 2004.
- [37] R.-C. R. HEDREA and E. M. PETRIU, "Evolving Fuzzy Models of Shape Memory Alloy Wire Actuators," *Science and Technology*, vol. 24, no. 4, pp. 353-365, 2021.
- [38] K. Kufieta and J. T. Gravidahl, "Force estimation in robotic manipulators: Modeling, simulation and experiments," *Department of Engineering Cybernetics NTNU Norwegian University of Science and Technology*, 2014.
- [39] S. L. Brunton, J. L. Proctor, and J. N. Kutz, "Sparse identification of nonlinear dynamics with control (SINDYc)," *IFAC-PapersOnLine*, vol. 49, no. 18, pp. 710-715, 2016.
- [40] M. Gautier and P. Poignet, "Extended Kalman filtering and weighted least squares dynamic identification of robot," *Control Engineering Practice*, vol. 9, no. 12, pp. 1361-1372, 2001.
- [41] J. Tao, B. Ye, Y. Xie, X. Tang, and B. Song, "Dynamic modeling and load identification of industrial robot using improved particle swarm optimization," in *2018 IEEE/ASME International Conference on Advanced Intelligent Mechatronics (AIM)*, 2018: IEEE, pp. 75-80.
- [42] J. Jin and N. Gans, "Parameter identification for industrial robots with a fast and robust trajectory design approach," *Robotics and Computer-Integrated Manufacturing*, vol. 31, pp. 21-29, 2015.
- [43] M. W. Spong, S. Hutchinson, and M. Vidyasagar, *Robot modeling and control*. John Wiley & Sons, 2020.
- [44] R. S. Andersen, "Kinematics of a UR5," *Aalborg University: Aalborg, Denmark*, 2018.
- [45] G. Porcelli, "Dynamic parameters identification of a UR5 robot manipulator," Politecnico di Torino, 2020.
- [46] A. Raviola, A. D. Martin, R. Guida, S. Pastorelli, S. Mauro, and M. Sorli, "Identification of a UR5 collaborative robot dynamic parameters," in *International Conference on Robotics in Alpe-Adria Danube Region*, 2021: Springer, pp. 69-77.

- [47] R. Kang, H. Chanal, T. Bonnemains, S. Pateloup, D. T. Branson, and P. Ray, "Learning the forward kinematics behavior of a hybrid robot employing artificial neural networks," *Robotica*, vol. 30, no. 5, pp. 847-855, 2012.
- [48] E. Kayacan and M. A. Khanesar, *Fuzzy neural networks for real time control applications: concepts, modeling and algorithms for fast learning*. Butterworth-Heinemann, 2015.
- [49] N. Kovincic, A. Müller, H. Gattringer, M. Weyrer, A. Schlotzhauer, and M. Brandstötter, "Dynamic parameter identification of the Universal Robots UR5," in *Proceedings of the ARW & OAGM Workshop*, 2019, pp. 44-53.
- [50] T. Söderström and P. Stoica, *System identification*. Prentice-Hall International, 1989.
- [51] L. Ljung, "System identification," in *Signal analysis and prediction*: Springer, 1998, pp. 163-173.
- [52] S. L. Kukreja, J. Löfberg, and M. J. Brenner, "A least absolute shrinkage and selection operator (LASSO) for nonlinear system identification," *IFAC proceedings volumes*, vol. 39, no. 1, pp. 814-819, 2006.
- [53] C. De Mol, E. De Vito, and L. Rosasco, "Elastic-net regularization in learning theory," *Journal of Complexity*, vol. 25, no. 2, pp. 201-230, 2009.
- [54] M. T. Hagan, H. B. Demuth, and M. Beale, *Neural network design*. PWS Publishing Co., 1997.
- [55] B. M. Wilamowski and H. Yu, "Improved computation for Levenberg-Marquardt training," *IEEE transactions on neural networks*, vol. 21, no. 6, pp. 930-937, 2010.
- [56] K. Kufieta, "Force estimation in robotic manipulators: Modeling, simulation and experiments," *Department of Engineering Cybernetics NTNU Norwegian University of Science and Technology*, 2014.
- [57] M. Ahmadihkhanesar, "UR5 collaborative robot static anti-gravity torque versus joint angle data," 2023.
- [58] J. Krmar, M. Vukićević, A. Kovačević, A. Protić, M. Zečević, and B. Otašević, "Performance comparison of nonlinear and linear regression algorithms coupled with different attribute selection methods for quantitative structure-retention relationships modelling in micellar liquid chromatography," *Journal of Chromatography A*, vol. 1623, p. 461146, 2020.
- [59] C.-T. Kim, J.-J. Lee, and H. Kim, "Variable projection method and Levenberg-Marquardt algorithm for neural network training," in *IECON 2006-32nd Annual Conference on IEEE Industrial Electronics*, 2006: IEEE, pp. 4492-4497.
- [60] S. Wang, X. Shao, L. Yang, and N. Liu, "Deep learning aided dynamic parameter identification of 6-DOF robot manipulators," *IEEE Access*, vol. 8, pp. 138102-138116, 2020.
- [61] M. Huang, X. Zhou, T. Huang, C. Yang, and W. Gui, "Dynamic optimization based on state transition algorithm for copper removal process," *Neural Computing and Applications*, vol. 31, no. 7, pp. 2827-2839, 2019.



M. A. Khanesar (M'07, SM'16) received the B.S., M.S., and Ph.D. degrees in control engineering from the K. N. Toosi University of Tech., Tehran, Iran, in 2005, 2007 and 2012. He is currently a research fellow with the University of Nottingham, UK. His current research interests include metrology, robotic, and control.



Minrui Yan is currently a Ph.D. student in the faculty of engineering, manufacturing metrology team, the University of Nottingham. He received his bachelor's degree in control technology from the Northwestern Polytechnical University, Xi'an, China, and master's degree in engineering from the University of

Southampton, Southampton, U.K. He is now working on modelling nonlinear robotic systems.



Wahyudin P. Syam was a research fellow at NARLy and MMT group at University of Nottingham. Wahyudin does research in dimensional metrology, Surface metrology, Software Engineering, Algorithms and Quality Assurance Engineering. Currently, he works at GMV innovating solution as a researcher and software engineer in satellite-based positioning solutions.



Samanta Piano is an Associate Professor in the faculty of engineering, manufacturing metrology team, the University of Nottingham. Her current research interest concerns the development of innovative and unconventional optical techniques and 3D probing systems for high-precision coordinate metrology to be used in industrial applications.



Richard K. Leach received his Ph.D. and D.Sc. degrees in surface metrology from the University of Warwick, Coventry, U.K., in 2000 and 2014, respectively. He spent 25 years at the National Physical Laboratory, Teddington, U.K. He is currently a professor of metrology with the University of Nottingham, Nottingham, U.K. He is also a Visiting Professor with Loughborough University, and the Harbin Institute of Technology, China.



David T. Branson, III received his bachelor's and master's degrees in mechanical engineering from the University of Wisconsin-Madison, Madison, WI, USA, and Ph.D. degree from the University of Bath, UK. He is currently a Professor of Dynamics and Control at the University of Nottingham, UK, and Director of the Nottingham Advanced Robotics Laboratory.